



OPEN

Altered static and dynamic intrinsic brain activity patterns in type 2 diabetic patients

Yongsheng Liang¹, Weiyin Vivian Liu², Mingrui Li³, Qingzhi Feng⁴, Shouchao Wei⁵, Wenjia Yang⁶, Zihua Guan⁶, Jie Li⁷, Wei Wei⁸, Meilian Li¹ & Hailing Zhou¹✉

Type 2 diabetes mellitus (T2DM) is a metabolic disorder characterized by chronic hyperglycemia resulting from insulin secretion and/or resistance. This study investigated intrinsic brain activity alterations using static and dynamic resting-state fMRI metrics in 65 T2DM patients versus 60 healthy controls. We analyzed fractional amplitude of low-frequency fluctuations (fALFF), dynamic fALFF (dfALFF) and dynamic functional stability (DFS). The T2DM group exhibited increased fALFF in the left inferior temporal gyrus and left fusiform gyrus and decreased fALFF in the bilateral precuneus, medial superior frontal gyrus, left inferior parietal lobule, and right supramarginal gyrus when compared with health controls. The T2DM group also showed increased dfALFF in the bilateral precuneus, left inferior parietal lobule, and right middle frontal gyrus. Moreover, the T2DM group exhibited decreased DFS in the bilateral precuneus, supramarginal gyrus, and left middle frontal gyrus, while the left cuneus showed increased dynamic stability. In the T2DM group, montreal cognitive assessment (MoCA) scores correlated negatively with glycated hemoglobin A_{1c} (HbA_{1c}) and fasting blood glucose (FBG), and positively with right supramarginal gyrus activity in both fALFF and DFS difference regions. Multiple brain regions exhibiting fALFF and DFS alterations showed negative correlations with fasting blood glucose and total cholesterol. These findings indicate that T2DM brain activity demonstrates a distinctive “low-intensity, highly-fluctuating, and destabilized” pattern, suggesting complex neural network dysfunction beyond simple functional suppression.

Keywords Type 2 diabetes, Functional magnetic resonance imaging, Fractional amplitude of low-frequency fluctuations, Dynamic fractional amplitude of low-frequency fluctuations, Dynamic stability

Type 2 diabetes mellitus (T2DM) is a metabolic disorder characterized by chronic hyperglycemia, resulting from insufficient insulin secretion and/or insulin resistance. The hyperglycemic state in T2DM not only accelerates brain aging and promotes neurodegenerative changes¹, but also progressively leads to a range of neurological consequences from cognitive impairment to dementia, accompanied by various systemic complications. It affects approximately 450 million adults worldwide, significantly impairing their quality of life².

Blood oxygenation level dependent (BOLD) based neuroimaging biomarkers such as amplitude of low-frequency fluctuation (ALFF), which reflects the intensity of spontaneous neuron fluctuations at low frequencies, can be used to identify brain regions that show changes in intrinsic brain activity (IBA) in pathological states³. ALFF is promising tools for early detection of subtle brain functional changes preceding macroscopic structural neuropathology and behavioral symptoms and risk stratification in long-spanning neurodegenerative and neuropsychological disorders⁴⁻⁷. However, ALFF is susceptible to physiological noise around the ventricles while the ratio of the low-frequency power spectrum to the total power spectrum over the entire frequency range (fractional ALFF, fALFF) represents the low-frequency oscillations characterized by the inhibition of non-specific signals in the ventricles had higher specificity and sensitivity of spontaneous neural activity in local brain regions⁸. This technical refinement provides a more comprehensive characterization of functional brain changes, establishing fALFF as a superior biomarker for neuropathological investigations.

¹Department of Radiology, Central People's Hospital of Zhanjiang, Zhanjiang, China. ²GE Healthcare, MR Research, Beijing, China. ³Department of Radiology, Zhanjiang First Hospital of Traditional Chinese Medicine, Zhanjiang, China. ⁴Physical Examination Centre, Central People's Hospital of Zhanjiang, Zhanjiang, China. ⁵Zhanjiang Institute of Clinical Medicine, Central People's Hospital of Zhanjiang, Zhanjiang, China. ⁶Department of Clinical Laboratory, Central People's Hospital of Zhanjiang, Zhanjiang, China. ⁷Department of Endocrinology, Central People's Hospital of Zhanjiang, Zhanjiang, China. ⁸Gaomi People's Hospital, Weifang, China. ✉email: ZHL13590049931@163.com

Emerging evidence demonstrates distinct fALFF patterns in neurological disorders compared to healthy controls^{9–15}. Nevertheless, research on fALFF alterations in T2DM-related brain injury remains limited. Notable findings include Bao et al.'s report of increased fALFF in the left superior temporal gyrus and the left auxiliary motor area alongside decreased activity in the left anterior central gyrus and the left middle frontal gyrus in T2DM group¹⁶. Similarly, Li et al. observed elevated fALFF in bilateral hippocampus of T2DM patients may represent an adaptive compensation mechanism for cognitive decline¹⁷. Despite these insights, current studies remain scarce and underpowered.

Conventional resting-state fMRI analyses typically assume static functional states by averaging signals across entire time series. However, intrinsic brain activity exhibits dynamic temporal fluctuations that are essential for functional integration and environmental adaptation¹⁸. Sliding-window approaches enable quantification of dynamic intrinsic brain activity indices, revealing time-dependent neural variations obscured by static analyses¹⁹. Based on this principle, the temporal variability of the BOLD signal plays a key role in the realization of various physiological functions of the nervous system. Dynamic fALFF (dfALFF) has been successfully applied across diverse neurological conditions including diffuse axonal injury, disorders of consciousness, epilepsy, Alzheimer's disease, psychiatric disorders, subcortical ischemic vascular disease, and unilateral sudden sensorineural hearing loss^{9–11,13,14,20,21}. The brain dynamically integrates, coordinates, and responds to internal and external stimuli; thus, maintaining the stability of neural activity and connectivity is essential for consciousness. However, when certain brain regions are damaged by external factors and their stability is compromised, other unaffected regions may attempt to compensate for the overall functional deficit by "overworking" or "altering their operational mode"²². The stability of voxel-based functional pattern highlights the inconsistency of the dynamic functional connections over time in psychiatric diseases and amyotrophic lateral sclerosis^{22–24}. Pertinently, Li et al. identified both decreased stability and increased variability in specific brain regions of T2DM patients²⁵, yet dynamic functional stability(DFS) changes in T2DM-related cognitive impairment remain unexplored.

This study investigates static and dynamic brain activity alterations in T2DM through fALFF and dfALFF analyses, with particular focus on DFS changes. Our work aims to elucidate novel mechanisms underlying T2DM-associated cognitive impairment from a temporal dynamics perspective.

Materials and methods

Participants

Participants enrolled in this study through the Department of Endocrinology and Health Examination Center at our hospital between November 2022 and January 2024. The study was approved by the Institutional Ethical Committee of Central People's Hospital of Zhanjiang, in compliance with the Declaration of Helsinki guidelines (KY20220124-07). All participants provided informed consent before inclusion in the study.

The diagnosis of type 2 diabetes was conducted by an endocrinologist according to the American Diabetes Association guidelines². Healthy individuals underwent a thorough physical examinations. Exclusion criteria were age lower than 18 years or higher than 65 years, presence of organic central nervous system diseases, hypertension and cardiovascular complications, noticeable hearing or visual impairments, pregnant, or breastfeeding, a history of mental illness, family history, severe head trauma, severe hypoglycemia, alcohol dependence or substance abuse, consumption of contraceptives at the time of the study, and individuals with contraindications for MRI. Demographic data, including gender, age, and education, were also collected. A total of 65 patients with T2DM and 60 healthy controls (HCs) were enrolled in this study.

Laboratory testing

The biochemical indices of T2DM patients encompass glycated hemoglobin A_{1c} (HbA_{1c}), fasting blood glucose (FBG), triglyceride (TG), total cholesterol (TC), and low-density lipoprotein (LDL) levels.

Cognitive testing

All participants completed a series of neuropsychological tests, including the montreal cognitive assessment (MoCA)²⁶ and the digital span test (DST) with both forward and backward tasks²⁷. These tests required 5 to 10 min for completion.

MRI acquisition

MRI data were acquired on a 3.0T MRI scanner (SIGNA Pioneer, GE Healthcare) using a twenty-one-channel phased array head coil. A set of routine imaging including axial T1-weighted, T2-weighted, and T2-fluid attenuated inversion recovery (T2-FLAIR) were acquired to exclude structural brain lesions. Subsequently, rs-fMRI (rs-fMRI parameters: flip angle = 90.0°, bandwidth = 250.0 kHz, TR = 2000 ms, TE = 30.0 ms, slices = 48.0, thickness = 3.0 mm, pixel size = 3.0 × 3.0 × 3.0 mm³, FOV = 256 × 256 mm², and NEX = 1) and high-resolution T1-weighted Brain volume image (3D-T1-BRAVO) (flip angle = 12.0°, bandwidth = 31.25 kHz, TR = 7.8 ms, TE = 3.1 ms, slices = 1024.0, thickness = 1.0 mm, pixel size = 1.0 × 1.0 × 1.0 mm³, FOV = 25.6 × 25.6 cm², and NEX = 1) were conducted.

Small-vessel disease assessment

Quantitative assessment of white matter degeneration and lacunar infarcts was conducted on T2-FLAIR sequences using the age-related white matter changes (ARWMC) scale²⁸. Participants with a score exceeding 2 were excluded from subsequent analyses. The scoring was performed independently by two experienced radiologists who were blinded to the group assignment. Inter-rater discrepancies were resolved through consensus review.

Image processing

Resting-state fMRI data preprocessing was performed using SPM12 and DPABI toolkits implemented in MATLAB. Processing steps included data format conversion, removal of the initial 10 time points, the time correction, head movement correction, regression of covariates, spatial standardization, and filtering²⁹. The preprocessing pipeline aimed to enhance image quality, reduce confounding factors, and prepare data for subsequent analysis.

Calculation of fALFF and DfALFF

The fALFF and dfALFF were computed using the Data Processing Assistant for Resting-State fMRI toolkit (DPARSF) and the Temporal Dynamic Analysis (Volume-based) toolkits within DPABI. Frequency filtering (0.01–0.1 Hz bandpass) was applied post-calculation³⁰. Sliding-window analysis was used to calculate the temporal dynamic characteristics of fALFF, dfALFF, using a window width = 64 s and a sliding step length = 4 s. To further validate the robustness and reliability of the dfALFF results, we conducted additional verification analyses using different parameter settings (window length = 50 s, step size = 4 s).

Calculation of dynamic functional stability

DFS calculated was performed using volumetric-based stability analysis toolkit in DPABI. DFS for each voxel in the brain was defined as the consistency of changes in dynamic functional connectivity (DFC) over time with the entire brain. We computed DFC using a sliding time window approach applied to consecutive data segments, with a window width of 64 s and a step size of 4 s. The analysis used a voxel-to-brain area approach, a method validated for its accuracy in previous studies²⁴. Brain structure was segmented into 200 regions using Craddock's 200 template³¹. Fisherz transform was used to improve the normality of the Kendall consistency coefficient (KCC) and all rs-MRI metric maps were smoothed (FWHM = 6 mm) to enhance the signal-to-noise ratio.

Statistical analysis

Statistical analysis was conducted using SPSS Statistics(IBM, SPSS, version 25). An independent two-sample t-test or Mann-Whitney test was employed for continuous variables in a normal or non-normal distribution. Categorical variables were compared using the χ^2 test. The significance level was set at $P < 0.05$. A two-sample t-test in DPABI software was employed to compare rs-MRI index images between the two groups using the built-in in BrainMask ($61 \times 73 \times 61$) as a template, covariates including gender, age, education, and average head motion parameters, and Gaussian random field (GRF) correction. Voxel p-value was set to < 0.001 and cluster p-value was set to < 0.05 . Statistically significant cluster volumes, peak MNI coordinates, and T-values were recorded based on the automated anatomical labeling (AAL) partition template. Subsequently, average parameter values of statistically significant clusters were extracted for further correlation analysis.

Partial correlation analysis was employed to determine the correlation between MoCA scores, clinical measurements, and the mean parameter values of the significant clusters in the T2DM group. A significance level of $P < 0.05$ was considered statistically significant.

Results

Demographics, clinical measurements, and cognitive testing

No significant differences were observed in gender, age, and education between the two groups while the T2DM group demonstrated significantly lower MoCA scores compared to the HC group (Table 1).

Differences in fALFF between T2DM and HCs

Following correction for multiple comparisons using the GRF method, the T2DM group exhibited increased fALFF in the left inferior temporal gyrus and left fusiform gyrus and decreased fALFF in the bilateral precuneus, medial superior frontal gyrus, left inferior parietal lobule, and right supramarginal gyrus when compared with health control (Table 2; Figs. 1 and 2).

	T2DM (n=65)	HC (n=60)	Statistics	P value
Age (years)	51.35 ± 9.90	50.88 ± 7.16	t = 0.302	0.763
Sex (female/male)	22/43	26/34	$\chi^2 = 1.187$	0.276
Education (years)	12.00(9.00;15.00)	12.00(9.00;12.00)	$z = -1.516$	0.130
HbA1c (%)	8.65(7.17;10.38)	N/A	N/A	N/A
FBG (mmol/L)	7.80(6.85;10.45)	N/A	N/A	N/A
TG (mmol/L)	1.97(1.01;2.58)	N/A	N/A	N/A
TC (mmol/L)	5.19(4.21;6.29)	N/A	N/A	N/A
LDL (mmol/L)	3.06(2.53;4.01)	N/A	N/A	N/A
MoCA	26.00(24.00;27.00)	27.00(26.00;28.00)	$z = -4.030$	< 0.001*
DST(forward)	8.00(8.00;9.00)	8.00(7.00;9.00)	$z = -0.695$	0.487
DST(inverse)	4.00(3.00;5.00)	4.00(3.00;4.00)	$z = -0.933$	0.351

Table 1. Demographic data, clinical biochemical indicators and neuropsychological result of all subjects.

Indicator	Cluster	MNI coordinates			Voxels	t-value	Brain regions
		X	Y	Z			
fALFF	1	-33	-6	-30	324	5.3376	Temporal_Inf_L Fusiform_L
	2	9	-66	39	562	-5.3437	Precuneus_R Precuneus_L
	3	-57	-51	33	401	-6.3223	Parietal_Inf_L
	4	42	-60	18	525	-5.9321	Supra_Marginal_R
	5	21	39	36	937	-6.0788	Frontal_Sup_Medial_L Frontal_Sup_Medial_R
Dynamic fALFF	1	-33	-75	33	214	4.3562	Parietal_Inf_L
	2	24	36	39	249	5.1002	Frontal_Mid_R
	3	-9	-51	30	653	4.9648	Precuneus_L Precuneus_R
Dynamic stability	1	9	-39	33	552	-5.5626	Precuneus_R Precuneus_L
	2	-45	21	36	335	-5.4834	Frontal_Mid_L
	3	-3	-81	42	390	5.855	Cuneus_L
	4	66	-39	27	213	-6.0001	Supra_Marginal_R
	5	-63	-42	33	168	-6.1574	Supra_Marginal_L

Table 2. Differences in fALFF, DfALFF and dynamic stability between T2DM and HCs.

Differences in DfALFF and DFS between T2DM and HCs

The T2DM group exhibited increased DfALFF in four clusters compared to the HC group. These clusters encompassed the bilateral precuneus, left inferior parietal lobule, and right middle frontal gyrus (Table 2; Fig. 1). The T2DM group exhibited decreased DFS in five clusters compared to the HC group, including the bilateral precuneus, supramarginal gyrus, and left middle frontal gyrus. Conversely, increased DFS was observed in the left cuneus (Table 2; Fig. 1).

To further validate the robustness and reliability of the results, we conducted additional verification analyses using different parameter settings (window length = 50 s, step size = 4 s). The results demonstrated that the location of the peak MNI coordinate and its corresponding cluster remained consistent, although the cluster size showed slight variations (Supplementary Tables 1 and Supplementary Fig. 1).

Partial correlation analysis

In the T2DM group, MoCA score exhibited negative correlations with glycated hemoglobin A_{1c} (HbA_{1c}) and FBG, respectively (Fig. 3). MoCA scores were positively correlated with the right supramarginal gyrus both in regions where fALFF differences were observed and where DFS differences were detected (Fig. 4). Furthermore, in the T2DM group, regions exhibiting fALFF differences including the bilateral precuneus, medial superior frontal gyrus, left inferior parietal lobule and right supramarginal gyrus showed negative correlations with FBG and TC (Figs. 4 and 5). Similarly, regions with DFS differences namely the bilateral precuneus, supramarginal gyrus and left middle frontal gyrus were also negatively correlated with FBG and TC (Figs. 4 and 5).

Discussion

Our study demonstrated altered spontaneous intrinsic brain activity in T2DM patients under static conditions, characterized by elevated fALFF in the left inferior temporal gyrus and left fusiform gyrus and decreased activity in the bilateral precuneus, medial superior frontal gyrus, left inferior parietal lobule, and right supramarginal gyrus. As a validated biomarker, fALFF sensitively reflects both enhancement and suppression of spontaneous neural activity through increased or decreased values, respectively^{8,10–17}.

It is noteworthy that the brain regions exhibiting altered spontaneous neural activity in T2DM substantially overlap with the default mode network (DMN). As a core network active during rest and internal cognitive processes, the DMN plays crucial roles in higher-order cognitive functions such as contextual decision-making, working memory, and social cognition³². Reduced DMN activity is associated with cognitive impairment and slower response to social stimuli, as evidenced by multimodal neuroimaging studies^{33–35}. Our data revealed decreased fALFF values in several regions of the DMN, including the bilateral precuneus, bilateral medial superior frontal gyrus, left inferior parietal lobule, and right supramarginal gyrus. These reductions were significantly negatively correlated with FBG levels. Consistent with these neural alterations, T2DM patients showed lower MoCA scores compared to the control group, and reduced fALFF in the right supramarginal gyrus was associated with MoCA decline in T2DM. These findings suggest that hyperglycemia may impair cognitive function in T2DM through dysfunction of critical neural circuits within the DMN.

Patients with T2DM exhibit reduced spontaneous neural activity in multiple brain regions, primarily associated with insulin resistance, hyperglycemic toxicity, and vascular injury. Insulin resistance impairs cerebral

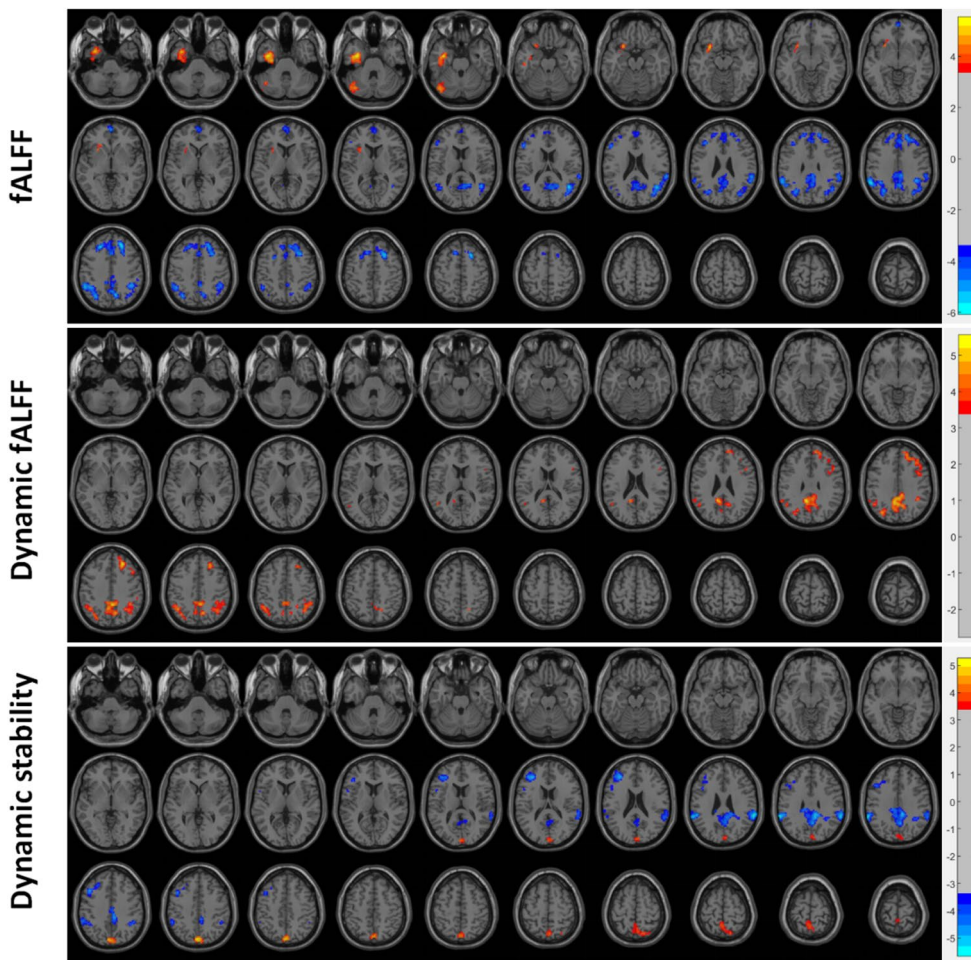


Fig. 1. A 64-s window and a 4-s step size were used to compute the temporal dynamic properties. Compared with the control group, T2DM patients showed significant differences in brain regions regarding the three metrics: fALFF, dynamic fALFF, and dynamic stability.

glucose utilization, leading to neuronal energy deficiency and suppressed electrical activity³⁶. Hyperglycemia promotes the formation of advanced glycation end products (AGEs), which trigger inflammatory pathways and damage mitochondria and cell membranes³⁷. T2DM also compromises vascular endothelial function, reduces nitric oxide release, and results in thickening of the microvascular basement membrane, capillary rarefaction, and decreased cerebral blood flow³⁸. Neurotransmitter dysregulation is also involved, exemplified by decreased choline acetyltransferase activity impairing learning and memory, and dysregulation of the glutamate/GABA system leading to neuronal apoptosis and loss of network synchrony³⁹. Furthermore, studies have indicated that hyperinsulinemia induced by T2DM may promote the deposition of amyloid-beta (A β) and the hyperphosphorylation of Tau protein, thereby exacerbating the pathological progression of Alzheimer's disease (AD)⁴⁰. This study also identified increased fALFF values in the left inferior temporal gyrus and left fusiform gyrus, suggesting possible compensatory mechanisms. These may include functional activation of higher-order visual and cognitive regions following partial neural damage, or overactivity in insulin receptor-dense areas to counteract energy deficit⁴¹. Abnormal vascular regulation and neurovascular uncoupling may also contribute to signal alterations⁴². These findings highlight the complexity of cerebral functional alterations in T2DM, indicating that heterogeneous patterns of neural activity may emerge across different brain regions and disease stages. Further longitudinal studies are needed to clarify the predictive value of these changes for cognitive decline.

From a dynamic perspective, bilateral precuneus, left inferior parietal lobule, and right middle frontal gyrus exhibit increased variability in spontaneous brain activity. It is noteworthy that these regions with high variability spatially correspond to those demonstrating reduced static activity. Elevated dfALFF in a brain region indicates its inability to maintain stable neural activity. We propose that this high dynamic variability may reflect a state of decompensation following compensatory efforts. Chronic hyperglycemia in T2DM causes prolonged impairment and suppression of certain brain regions. When exposed to various external stimuli, brain areas with reduced fALFF may enhance their dynamic flexibility and variability to effectively compensate and rapidly stabilize the functionally compromised regions. However, such compensation is not always effective or stable. In some brain regions with decreased fALFF, increased dfALFF may indicate inefficient, unstable, or even disruptive inputs or

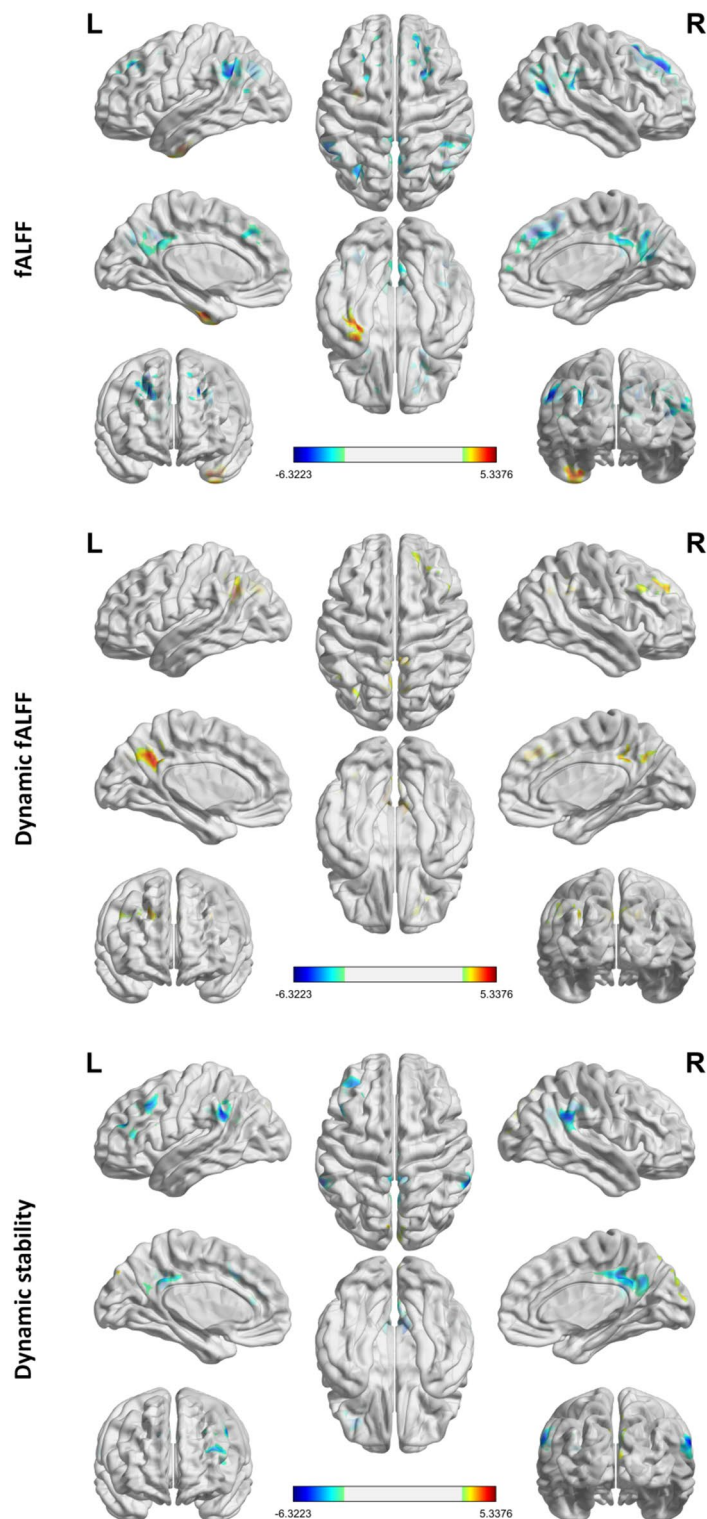


Fig. 2. 3D renderings: there are significant differences in the three indicators of fALFF, dynamic fALFF and dynamic stability in the brain regions of T2DM patients.

modulation from other areas. Rather than providing effective compensation, these maladaptive interactions may introduce additional fluctuations⁴³. Furthermore, significantly lower MoCA scores in T2DM patients compared to controls highlight the inadequacy of this adaptation in maintaining overall cognitive function.

Additionally, a decrease in DFS reflects a failure in the overall regulation of network function and an impairment in the coordination of information across regions, which is essential for conscious processing. Our findings align with emerging evidence indicating that temporal instability in functional hierarchy contributes

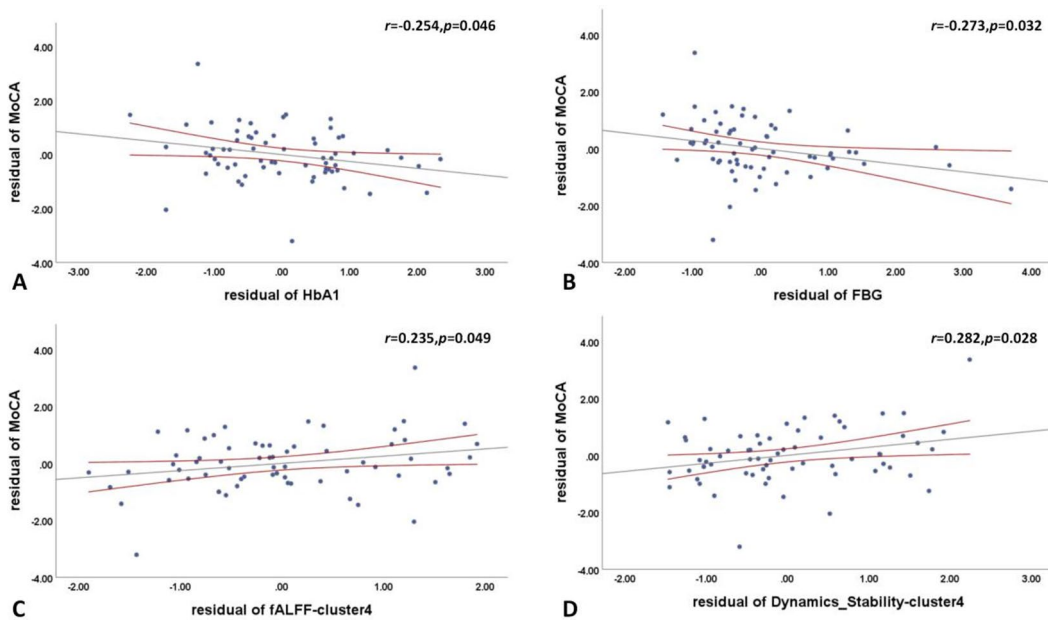


Fig. 3. In the T2DM group, MoCA score exhibited negative correlations with HbA_{1c} and FBG (A, B), respectively. MoCA scores were positively correlated with the right supramarginal gyrus both in regions where fALFF differences were observed and where DFS differences were detected (C, D).

to cognitive fragmentation in neuropsychiatric disorders^{24,44}, suggesting shared pathophysiological pathways between diabetes and primary neurodegenerative diseases. In our T2DM cohort, decreased DFS was observed in the bilateral precuneus, supramarginal gyrus, and left middle frontal gyrus, and these reductions were negatively correlated with FBG levels. Concurrently, DFS values in the right supramarginal gyrus were positively correlated with MoCA scores. This decline in dynamic stability corresponds clinically to fluctuating and impaired cognitive function in T2DM patients. Notably, static, dynamic, and DFS analyses revealed abnormalities in overlapping brain regions among our T2DM participants. In summary, the observed decrease in static fALFF coupled with reduced dynamic stability in certain brain regions among T2DM patients suggests a state of functional destabilization, where neural activity is characterized not only by diminished average intensity but also by impaired stability and coordination. This reflects that the cerebral impact of T2DM extends beyond mere “reduced function,” pointing rather to widespread dysregulation and disorganization within neural networks.

Our analysis revealed decreased DFS in the bilateral precuneus, supramarginal gyrus, and left middle frontal gyrus, alongside increased DFS in the left cuneus. Highly interconnected high-order association cortices, such as the DMN, exhibit enhanced temporal stability to facilitate sustained multimodal integration, whereas lower-order sensorimotor regions demonstrate greater dynamic flexibility to adapt to rapidly changing environmental demands²⁴. Previous studies have shown that ruminative states are characterized by reduced stability in the DMN and increased stability in the frontoparietal network (FPN) compared to baseline conditions⁴⁵. This network-specific reorganization of stability aligns with established transdiagnostic patterns wherein distinct psychiatric disorders exhibit unique DFS profiles across functional networks⁴⁶. Our findings extend this paradigm to diabetic encephalopathy by revealing distinct alterations in DFS: the “functional failure” of advanced brain regions may compel lower-order regions to compensate through “overworking” or “shifting operational modes” in an attempt to maintain overall neural function. While previous articles solely analyzed alterations in dynamic functional connectivity in T2DM²⁵, our study incorporates both static and dynamic analyses, with a particular focus on temporal variability metrics, such as dfALFF and DFS, offers a novel perspective for understanding functional changes in the T2DM brain. These metrics may capture early neural destabilization more sensitively, potentially even before significant changes in static fALFF become apparent.

Neuroimaging-metabolic correlation analyses revealed that regional alterations in fALFF and DFS are associated with both glycemic control and TC levels, which represents a significant and valuable finding. Previous studies have suggested that elevated total cholesterol exacerbates brain network dysfunction in T2DM patients through multiple pathways including vascular, inflammatory, and cellular mechanisms, synergizing with hyperglycemia to reduce neural activity intensity and stability⁴⁷. However, our study did not identify a mediating role of TC in diabetic cognitive impairment, which warrants further detailed investigation into this finding.

Several limitations should be noted in our study. Firstly, it is a cross-sectional design, our study needs a larger T2DM cohort including longitudinal follow-ups to confirm the changes of both fALFF, dALFF and DFS. Secondly, gender effect needs to be explored in a larger T2DM groups. Third, although gender was incorporated as a covariate in our analysis, whether there are differences in alterations of brain function between male and female patients remains undetermined. Future studies will aim to conduct analyses with better gender matching.

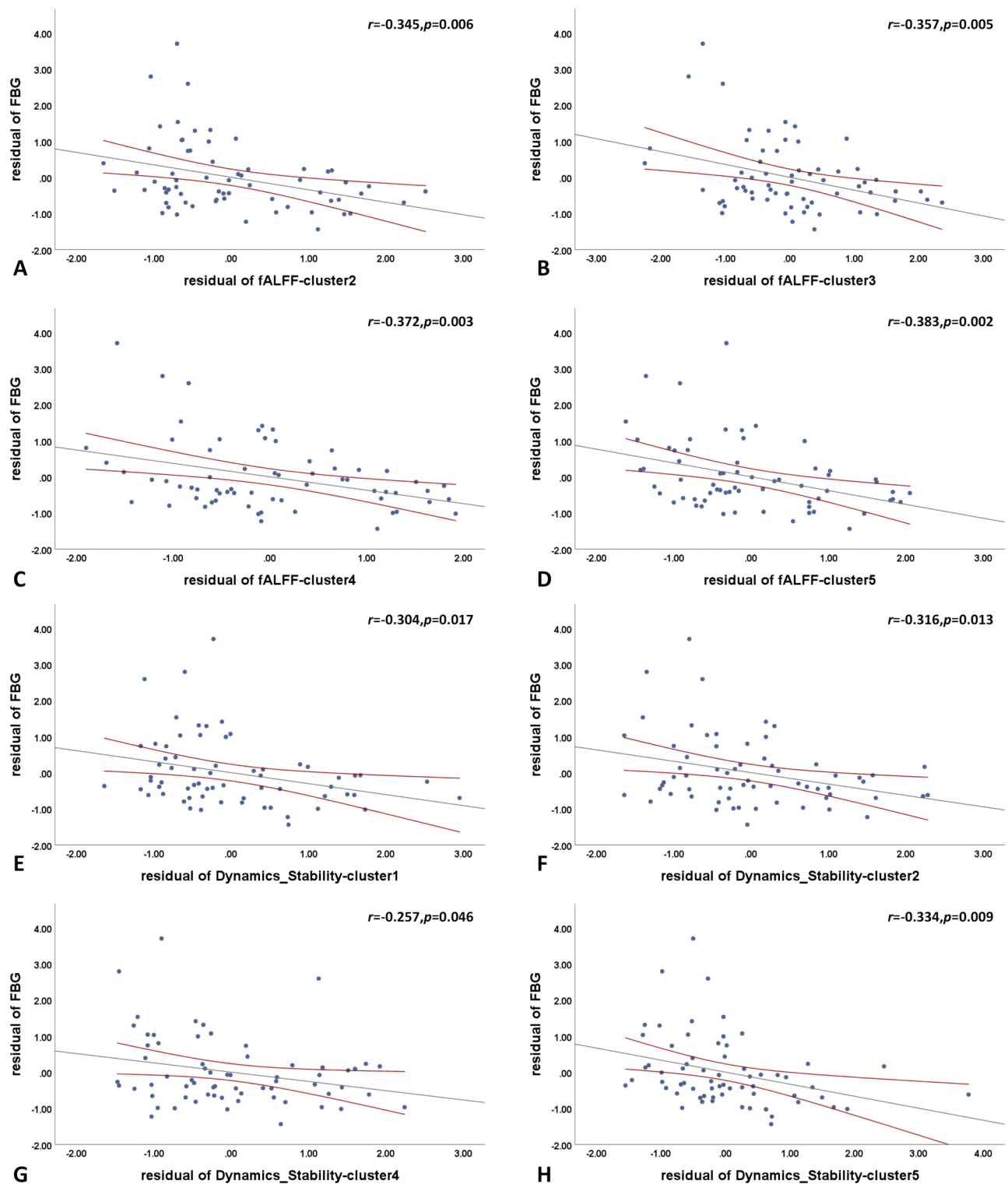


Fig. 4. In the T2DM group, regions exhibiting fALFF differences including the bilateral precuneus, medial superior frontal gyrus, left inferior parietal lobule and right supramarginal gyrus showed negative correlations with FBG (A, B, C, D). Similarly, regions with DFS differences namely the bilateral precuneus, supramarginal gyrus and left middle frontal gyrus were also negatively correlated with FBG (E, F, G, H).

Fourth, the types of anti-diabetic medications taken by patients were inconsistent, and whether this has an impact on cerebral function remains to be explored.

In summary, patients with T2DM exhibit a characteristic pattern of brain activity described as “low-intensity, high-fluctuation, and destabilized.” This reveals that cerebral impairment in T2DM extends beyond

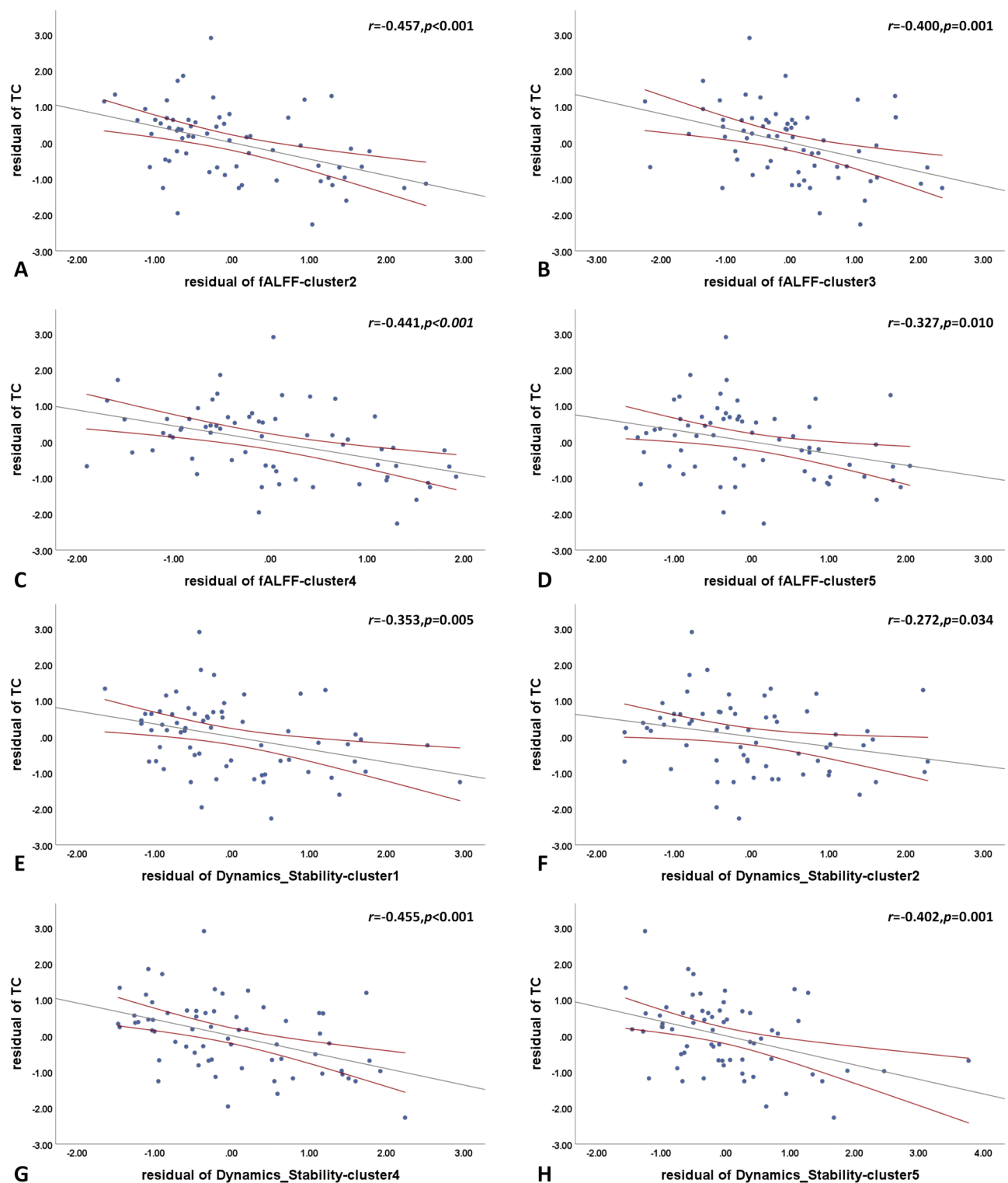


Fig. 5. In the T2DM group, regions exhibiting fALFF differences including the bilateral precuneus, medial superior frontal gyrus, left inferior parietal lobule and right supramarginal gyrus showed negative correlations with TC (A, B, C, D). Similarly, regions with DFS differences namely the bilateral precuneus, supramarginal gyrus and left middle frontal gyrus were also negatively correlated with TC (E, F, G, H).

simple functional suppression, reflecting instead a more complex state of neural network dysfunction and decompensation. Such intrinsic neural instability likely underlies the cognitive fluctuations and decline in executive function observed in these patients.

Data availability

The datasets used and/or analysed during the current study available from the corresponding author on reasonable request.

Received: 20 April 2025; Accepted: 27 November 2025

Published online: 08 December 2025

References

- Biessels, G. J., Nobili, F., Teunissen, C. E., Simó, R. & Scheltens, P. Understanding multifactorial brain changes in type 2 diabetes: a biomarker perspective. *Lancet Neurol.* **19**, 699–710. [https://doi.org/10.1016/s1474-4422\(20\)30139-3](https://doi.org/10.1016/s1474-4422(20)30139-3) (2020).
2. Diagnosis and classification of diabetes: standards of care in Diabetes-2024. *Diabetes Care.* **47**, S20–s42. <https://doi.org/10.2337/dc24-S002> (2024).
3. Zang, Y. F. et al. Altered baseline brain activity in children with ADHD revealed by resting-state functional MRI. *Brain Dev.* **29**, 83–91. <https://doi.org/10.1016/j.braindev.2006.07.002> (2007).
4. Yang, F. et al. A study of spontaneous brain activity on resting-state functional magnetic resonance imaging in adults with MRI-negative temporal lobe epilepsy. *Neuropsychiatr. Dis. Treat.* **18**, 1107–1116. <https://doi.org/10.2147/ndt.S366189> (2022).
5. Du, Y. Y. et al. Survivors of COVID-19 exhibit altered amplitudes of low frequency fluctuation in the brain: a resting-state functional magnetic resonance imaging study at 1-year follow-up. *Neural Regeneration Res.* **17**, 1576–1581. <https://doi.org/10.4103/1673-5374.327361> (2022).
6. Zhang, L., Wei, X. & Zhao, J. Amplitude of low-frequency oscillations in first-episode drug-naïve patients with major depressive disorder: A resting state functional magnetic resonance imaging study. *Neuropsychiatr. Dis. Treat.* **18**, 555–561. <https://doi.org/10.2147/ndt.S348683> (2022).
7. Lan, Y. et al. Resting-state functional magnetic resonance imaging study comparing tremor-dominant and postural instability/gait difficulty subtypes of Parkinson's disease. *Radiol. Med.* **128**, 1138–1147. <https://doi.org/10.1007/s11547-023-01673-y> (2023).
8. Zou, Q. H. et al. An improved approach to detection of amplitude of low-frequency fluctuation (ALFF) for resting-state fMRI: fractional ALFF. *J. Neurosci. Methods.* **172**, 137–141. <https://doi.org/10.1016/j.jneumeth.2008.04.012> (2008).
9. Zhang, L. et al. Three major psychiatric disorders share specific dynamic alterations of intrinsic brain activity. *Schizophr. Res.* **243**, 322–329. <https://doi.org/10.1016/j.schres.2021.06.014> (2022).
10. Zhou, F. et al. Characterizing static and dynamic fractional amplitude of low-frequency fluctuation and its prediction of clinical dysfunction in patients with diffuse axonal injury. *Acad. Radiol.* **28**, e63–e70 (2021). <https://doi.org/10.1016/j.acra.2020.02.020>
11. Yu, Y. et al. Disrupted strength and stability of regional brain activity in disorder of consciousness patients: A resting-state functional magnetic resonance imaging study. *Neuroscience* **469**, 59–67. <https://doi.org/10.1016/j.neuroscience.2021.06.031> (2021).
12. Wen, M. et al. More than just statics: Temporal dynamic changes of intrinsic brain activity in cigarette smoking. *Addict. Biol.* **26**, e13050. <https://doi.org/10.1111/adb.13050> (2021).
13. Song, C. et al. Static and temporal dynamic alteration of intrinsic brain activity in MRI-negative temporal lobe epilepsy. *Seizure* **108**, 33–42. <https://doi.org/10.1016/j.seizure.2023.04.004> (2023).
14. Lin, Y., Zeng, Q., Hu, M., Peng, G. & Luo, B. Temporal dynamic changes of intrinsic brain activity associated with cognitive reserve in prodromal Alzheimer's disease. *J. Alzheimer's Disease: JAD.* **81**, 1285–1294. <https://doi.org/10.3233/jad-201244> (2021).
15. Lv, L. et al. Assessing the effects of vitamin D on neural network function in patients with Parkinson's disease by measuring the fraction amplitude of low-frequency fluctuation. *Front. Aging Neurosci.* **13**, 763947. <https://doi.org/10.3389/fnagi.2021.763947> (2021).
16. Bao, Y. W. et al. The fractional amplitude of low-frequency fluctuations signals related to amyloid uptake in high-risk populations-A pilot fMRI study. *Front. Aging Neurosci.* **14**, 956222. <https://doi.org/10.3389/fnagi.2022.956222> (2022).
17. Li, M. et al. Changes in the structure, perfusion, and function of the hippocampus in type 2 diabetes mellitus. *Front. NeuroSci.* **16**. <https://doi.org/10.3389/fnins.2022.1070911> (2022).
18. Park, H. J., Friston, K. J., Pae, C., Park, B. & Razi, A. Dynamic effective connectivity in resting state fMRI. *NeuroImage* **180**, 594–608. <https://doi.org/10.1016/j.neuroimage.2017.11.033> (2018).
19. Allen, E. A. et al. Tracking whole-brain connectivity dynamics in the resting state. *Cereb. Cortex (New York, N.Y.)* **24**, 663–676 (1991). <https://doi.org/10.1093/cercor/bhs352> (2014).
20. Song, Z. et al. Altered static and dynamic indices of intrinsic brain activity in patients with subcortical ischemic vascular disease: a resting-state functional magnetic resonance imaging analysis. *Neuroradiology* **65**, 923–931. <https://doi.org/10.1007/s00234-023-03135-8> (2023).
21. Li, J. et al. Altered static and dynamic intrinsic brain activity in unilateral sudden sensorineural hearing loss. *Front. Neurosci.* **17**. <https://doi.org/10.3389/fnins.2023.1257729> (2023).
22. Zhu, J., Zhang, S., Cai, H., Wang, C. & Yu, Y. Common and distinct functional stability abnormalities across three major psychiatric disorders. *NeuroImage Clin.* **27**, 102352. <https://doi.org/10.1016/j.nicl.2020.102352> (2020).
23. Wei, J. et al. Abnormal stability of dynamic functional architecture in amyotrophic lateral sclerosis: A preliminary resting-state fMRI study. *Front. Neurol.* **12**, 744688. <https://doi.org/10.3389/fneur.2021.744688> (2021).
24. Li, L., Lu, B. & Yan, C. G. Stability of dynamic functional architecture differs between brain networks and states. *NeuroImage* **216**, 116230 (2020). <https://doi.org/10.1016/j.neuroimage.2019.116230>
25. Li, Y. et al. Altered dynamic functional architecture in type 2 diabetes mellitus. *Front. Endocrinol.* **13** <https://doi.org/10.3389/fend.0.2022.1117735> (2022).
26. Li, X. et al. The role of the Montreal cognitive assessment (MoCA) and its memory tasks for detecting mild cognitive impairment. *Neurol. Sciences: Official J. Italian Neurol. Soc. Italian Soc. Clin. Neurophysiol.* **39**, 1029–1034. <https://doi.org/10.1007/s10072-018-3119-0> (2018).
27. Diamond, A. Executive functions. *Ann. Rev. Psychol.* **64**, 135–168. <https://doi.org/10.1146/annurev-psych-113011-143750> (2013).
28. Wahlund, L. O. et al. A new rating scale for age-related white matter changes applicable to MRI and CT. *Stroke* **32**, 1318–1322. <https://doi.org/10.1161/01.str.32.6.1318> (2001).
29. Yan, C. G., Wang, X. D., Zuo, X. N. & Zang, Y. F. DPABI: Data processing & analysis for (resting-state) brain imaging. *Neuroinformatics* **14**, 339–351 (2016). <https://doi.org/10.1007/s12021-016-9299-4>
30. Yan, C. G., Yang, Z., Colcombe, S. J., Zuo, X. N. & Milham, M. P. Concordance among indices of intrinsic brain function: insights from inter-individual variation and temporal dynamics. *Sci. Bull.* **62**, 1572–1584. <https://doi.org/10.1016/j.scib.2017.09.015> (2017).
31. Craddock, R. C., James, G. A., Holtzheimer 3rd, P. E., Hu, X. P. & Mayberg, H. S. A whole brain fMRI atlas generated via spatially constrained spectral clustering. *Hum. Brain. Mapp.* **33**, 1914–1928. <https://doi.org/10.1002/hbm.21333> (2012).

32. Yeshurun, Y., Nguyen, M. & Hasson, U. The default mode network: where the idiosyncratic self meets the shared social world. *Nat. Rev. Neurosci.* **22**, 181–192. <https://doi.org/10.1038/s41583-020-00420-w> (2021).
33. Mohan, A. et al. The significance of the default mode network (DMN) in neurological and neuropsychiatric disorders: A review. *Yale. J. Biol. Med.* **89**, 49–57 (2016).
34. Deng, L. et al. Concomitant functional impairment and reorganization in the linkage between the cerebellum and default mode network in patients with type 2 diabetes mellitus. *Quant. Imaging Med. Surg.* **11**, 4310–4320. <https://doi.org/10.21037/qims-21-41> (2021).
35. Chen, Y. et al. Dysfunctional organization of default mode network before memory impairments in type 2 diabetes. *Psychoneuroendocrinology* **74**, 141–148. <https://doi.org/10.1016/j.psyneuen.2016.08.012> (2016).
36. Chen, W., Kullmann, S. & Rhea, E. M. Expanding the understanding of insulin resistance in brain and periphery. *Trends Endocrinol. Metab.* <https://doi.org/10.1016/j.tem.2025.04.010> (2025).
37. Chen, Y. et al. Advanced glycation end products and reactive oxygen species: Uncovering the potential role of ferroptosis in diabetic complications. *Mol. Med. (Cambridge Mass.)* **30**, 141. <https://doi.org/10.1186/s10020-024-00905-9> (2024).
38. Zelinskaya, I. et al. Vascular region-specific changes in arterial tone in rats with type 2 diabetes mellitus: opposite responses of mesenteric and femoral arteries to acetylcholine and 5-hydroxytryptamine. *Life Sci.* **286**, 120011. <https://doi.org/10.1016/j.lfs.2021.120011> (2021).
39. Liu, J. et al. Abnormal Glu/mGluR(2/3)/PI3K pathway in the hippocampal neurovascular unit leads to diabetes-related depression. *Neural Regeneration Res.* **16**, 727–733. <https://doi.org/10.4103/1673-5374.296418> (2021).
40. Xie, L. et al. Alzheimer's beta-amyloid peptides compete for insulin binding to the insulin receptor. *J. Neurosci.* **22** (Rc221). <https://doi.org/10.1523/JNEUROSCI.22-10-j0001.2002> (2002).
41. He, D. et al. Structural and functional brain abnormal alteration in patients with type 2 diabetes mellitus: A coordinate-based meta-analysis. *Transl Psychiatry.* **15**, 269. <https://doi.org/10.1038/s41398-025-03488-z> (2025).
42. Min, Y. et al. Retinal vessel diameter reflects altered resting-state fMRI connectivity and cognitive performance: A community-based study. *GeroScience* <https://doi.org/10.1007/s11357-025-01667-w> (2025).
43. Li, Y. L. et al. Alteration of the individual metabolic network of the brain based on Jensen-Shannon divergence similarity estimation in elderly patients with type 2 diabetes mellitus. *Diabetes* **71**, 894–905. <https://doi.org/10.2337/db21-0600> (2022).
44. Dehaene, S., Lau, H. & Kouider, S. What is consciousness, and could machines have it? *Science (New York N.Y.)* **358**, 486–492. <https://doi.org/10.1126/science.aan8871> (2017).
45. Chen, X. & Yan, C. G. Hypostability in the default mode network and hyperstability in the frontoparietal control network of dynamic functional architecture during rumination. *NeuroImage* **241**, 118427. <https://doi.org/10.1016/j.neuroimage.2021.118427> (2021).
46. Zhang, J. et al. Neural, electrophysiological and anatomical basis of brain-network variability and its characteristic changes in mental disorders. *Brain: J. Neurol.* **139**, 2307–2321. <https://doi.org/10.1093/brain/aww143> (2016).
47. Li, X. et al. Non-alcoholic fatty liver disease is associated with brain function disruption in type 2 diabetes patients without cognitive impairment. *Diabetes Obes. Metab.* **26**, 650–662. <https://doi.org/10.1111/dom.15354> (2024).

Author contributions

L. Y. participated in the writing of the article. L.V. provided guidance on the design and writing of the article. L.M. post-processed the images included in the study. F.Q., W.S., W.W., Y.W., G.Z., L.M., L.J. collected data. Z.H. is the guarantor of this study and is mainly responsible for the whole experiment process and the revision of the article.

Funding

The study was funded by the Medical Scientific Research Foundation of Guangdong Province (No. A2024369), the Project of Traditional Chinese Medicine Bureau of Guangdong Province (No. 20221444), the Scientific Research Project of Guangdong Provincial Bureau of Traditional Chinese Medicine (No. 20262075), the Guang-Dong Basic and Applied Basic Research Foundation (No. 2021A151515010827), the Zhanjiang Science and Technology Project (No. 2021A05115), the Weifang Health Commission Research Project (WFWSJK-2021-296), and the Doctoral Cooperation Project of Central People's Hospital of Zhanjiang (No. 2021H03).

Declarations

Competing interests

The authors declare no competing interests.

Additional information

Supplementary Information The online version contains supplementary material available at <https://doi.org/10.1038/s41598-025-30847-z>.

Correspondence and requests for materials should be addressed to H.Z.

Reprints and permissions information is available at www.nature.com/reprints.

Publisher's note Springer Nature remains neutral with regard to jurisdictional claims in published maps and institutional affiliations.

Open Access This article is licensed under a Creative Commons Attribution-NonCommercial-NoDerivatives 4.0 International License, which permits any non-commercial use, sharing, distribution and reproduction in any medium or format, as long as you give appropriate credit to the original author(s) and the source, provide a link to the Creative Commons licence, and indicate if you modified the licensed material. You do not have permission under this licence to share adapted material derived from this article or parts of it. The images or other third party material in this article are included in the article's Creative Commons licence, unless indicated otherwise in a credit line to the material. If material is not included in the article's Creative Commons licence and your intended use is not permitted by statutory regulation or exceeds the permitted use, you will need to obtain permission directly from the copyright holder. To view a copy of this licence, visit <http://creativecommons.org/licenses/by-nc-nd/4.0/>.

© The Author(s) 2025